Facile preparation of Ag nanocubes at 30°C under light irradiation

Danli Li, Yangyang Shan, Ruiyi Liu, Qian Wu, Tingting Zheng, Kai Li ✉

Department of Chemistry, Capital Normal University, Beijing 100048, People's Republic of China
✉ *E-mail: LK123LK@126.com*

Published in Micro & Nano Letters; Received on 11th October 2017; Revised on 29th November 2017; Accepted on 19th December 2017

Preparation of silver nanocubes (Ag NCs) with low temperature and controlled shapes is challenging in an aqueous solution because of its anticipated low embodied energy and experiment controllability. In this work, Ag NCs have been successfully synthesised under facile reaction conditions (at 30°C oil bath and under daylight illumination) by coordination effects of thermal reduction and photoinduced reduction. The obtained Ag NCs were characterised by transmission electron microscopy, UV–visible spectrophotometer and X-ray diffractometer. It turned out that, Ag NCs were prepared by using trifluoroacetic acid silver, cetyltrimethyl ammonium chloride, ascorbic acid, ferric chloride and sodium hydrosulphide as raw materials, and their sizes around 35 nm. Besides, as-synthesised Ag NCs with uniform size and high yield would serve as outstanding substrates for surface-enhanced Raman scattering detection, and as sacrificial templates to fabricate Au nanocages.

1. Introduction: Noble metal nanostructures have been the focus of research due to their unique properties useful in numerous applications [1]. Especially, silver nanoparticles (Ag NPs) have many potential applications in optical switches, molecular identification, catalysis and medical treatment [2–5]. Over the past decade, Ag NPs have been successfully synthesised with a large number of diversified shapes, such as spheres [6–8], cubes [9–14], bars [15] and so on. It is worth mentioning that silver nanocubes (Ag NCs) have been attracted much attention owing to its perfect surface-enhanced Raman scattering (SERS) performance and being used as a sacrificial template to generate gold, platinum and palladium nanocages. As a result, great efforts must be given to prepare Ag NCs with high quality and relatively large quantity [16]. In order to achieve the target, researchers have developed a number of methods to produce Ag NCs, with notable examples including polyol reduction [11], hydrothermal process [17, 18], epitaxial growth on Au octahedronal seeds [19] and ATP-mediated reduction in a polymer matrix [20]. However, most of these protocols have shortcomings in terms of size control, yield, quantity, as well as reproducibility [21].

In 2002, Xia's group prepared Ag NCs for the first time by polyol reduction [10]. In 2016, Ag NCs with small size of 15 nm were prepared by optimising the experimental conditions [14]. It is universally acknowledged that polyol reduction method has quite a few shortcomings, for example, large energy consumption, poor experimental controllability and so on. In the same year, Ag NCs were prepared based on previous aqueous phase methods, and the exciting breakthrough is the reaction temperature could be as low as 60°C at present. In this Letter, Ag NCs have been successfully synthesised under facile optimisation of reaction conditions (at 30°C oil bath and under daylight illumination) by coordination effects of thermal reduction and photoinduced reduction, which is according to a previously reported approach of Xia [22]. As trifluoroacetic acid silver (CF_3COOAg), cetyltrimethyl ammonium chloride (CTAC), ascorbic acid (AA) and ferric chloride ($FeCl_3$) were used as precursor, protective agent, reducing agent and oxidation etching agent, respectively, Ag NCs were prepared with their sizes about 35 nm using sodium hydrosulphide (NaHS) as nucleating auxiliary agent at 30°C under light irradiation. The target of synthesising Ag NCs with uniform size and high yield at low reaction temperature was achieved. Furthermore, a water-based synthesis was anticipated to be greener and more environment-friendly, offering more flexibility and convenience for execution [22]. Besides, as-synthesised Ag NCs with uniform size and high yield would serve as outstanding substrates for SERS detection of chemicals [23, 24], biological species [25], for molecular imaging, and for monitoring microorganisms [26] and cells [27].

2. Experiments

2.1. Materials: CF_3COOAg and CTAC were purchased from Alfa Aesar. AA, hydrochloric acid (HCl) and NaHS were obtained from Sigma-Aldrich. $FeCl_3$ was purchased from Sinopharm Chemical Reagent Co., Ltd. All chemicals were used as received without further treatment. Ultrapure deionised water (18.2 MΩ cm) was used throughout the experiments.

2.2. Synthesis of Ag NCs: Ag NCs with an edge length of about 35 nm were prepared according to Xia's group with a simple change [22]. Typically, a 50 ml round bottom flask containing 30 ml of 20 mM CTAC, 3 ml of 100 mM AA and 180 µl of 2.66×10^{-3} mM NaHS was placed in an oil bath set to 60°C and allowed to heat for 10 min, then 480 µl of 4.29×10^{-3} mM $FeCl_3$ and 300 µl of 10 mM CF_3COOAg were rapidly injected into the above solution which was allowed to proceed for 6 h under daylight illumination, finally, the reaction mixture was yellow-green. The flask was capped with a glass stopper except during the addition of reagents. In order to investigate the effects of reaction temperatures on preparing Ag NCs, the other parallel experiments were conducted following the same process as that of 60°C, except that the reaction temperature was set at 50, 40 and 30°C, respectively. As-synthesised Ag NCs in aqueous solution were cooled to room temperature and stored at 4°C for subsequent uses. Except that NaHS was freshly prepared, the remaining solution was incubated for 24 h before use.

2.3. Synthesis of further optimised Ag NCs: The synthesis of Ag NCs was carried out by following the procedure described in Section 2.2, except that the reducing agent was increased by two times. The sample collection was same as described in Section 2.2.

2.4. Characterisation: The morphologies of Ag NCs were characterised by Hitachi H-7650 transmission electron microscopy (TEM), with an accelerating voltage of 80 kV. First, irregular nanoparticles, nanowires and nanorods were removed by centrifugation at 2500 rpm for 10 min. Then Ag NCs in above suspension were collected by centrifugation at 10000 rpm for 10 min. After that, Ag NCs were ultrasonically treated for 90 s before 50 µl of the suspension were transformed onto a 3 mm diameter holey

doi: 10.1049/mnl.2017.0703

carbon-coated copper grid. The UV–visible (UV–Vis) spectra were taken using a Shimadzu 2700 spectrophotometer. The X-ray diffractometer (XRD, Bruke D8) equipped was used to identify relevant phases and preferred orientation.

3. Results and discussion

3.1. Effects of reaction temperatures: As shown by TEM images in Figs. 1*a*–*d*), the morphologies of the obtained Ag NCs are uniform under different reaction temperatures. The Ag NCs have an edge length of 80, 60, 45, 35 nm, respectively. The particle size and shape of Ag NCs were determined by electron microscopy. The controllable cubic shape develops due to using chloride ion (Cl^-) instead of polyvinyl pyrolidone (PVP) as a capping agent for the Ag {100} facets. Cl^- has a much smaller size than the long polymer chain of PVP. Thus, it can better cover the side faces to make the edges and corners sharp [22]. The synthesis was further optimised by adjusting volume of the reducing agent. In Figs. 1*e* and *f*, the yields of Ag NCs were obviously increased at the optimised conditions. As shown in Fig. 2*a*, the major localised surface plasmon resonance (LSPR) peaks of the Ag NCs display a continuous blue-shift along with the decrease of reaction temperatures. As the edge length of the Ag NCs was decreased from 80 to 60, 45 and 35 nm, the positions of the major LSPR peaks were located from 508 to 486, 466 and 458 nm, respectively. The plot in Fig. 2*b* suggests that there was a more or less linear relationship between the LSPR peak position and the edge length of the Ag NCs. The equation for describing the calibration curve was $\lambda_{max} = 1.1739L + 414.4348$ ($R^2 = 0.9970$), where λ_{max} and L are the peak position and edge length, respectively. In practice, this calibration curve should allow one to obtain Ag NCs of a specific edge length by monitoring the UV–Vis spectra of the reaction solution [21]. To validate the Miller indices for the exposed planes and their relative abundance, the XRD patterns were obtained and the diffraction intensity of selected planes to that of standard fcc Ag (JCPDF: 65-2871) is compared. In ideal isotropic fcc Ag, the (111) plane is the strongest peak and the intensity ratio of (111)/(200) is expected to be 2.5 [28]. According to the results reported by Sun and Xia [10], after the Miller indices for the six facets have been determined as {200} planes, edges are {110} planes and that the truncated corners crystallographic orientation suggests that the rounded become {111} planes. Notably, the atomic arrangement for the (200) planes in a fcc lattice is identical to that of (100) planes. As shown in Fig. 2*c*, Ag NCs were prepared under different reaction temperatures, which adopted a perfect cubic shape (Fig. 1), the (111) peak was negligible, whereas the predominant signal was due to the (200) plane. This result confirmed that the six facets were indeed {100} planes. Moreover, the ordered two-dimensional packing of NCs was presumed to strengthen the (200) signal considerably [28]. Therefore, we have successful synthesised Ag NCs with uniform size and high yields at 30°C.

3.2. Effects of NaHS: In order to synthesise Ag NCs with high yield, we optimised the experimental conditions by adjusting the concentration of NaHS while the other parameters were kept the same. As shown in Fig. 3, when the concentration of NaHS was 0 mM (without using), Ag NCs (Fig. 3*a*) were in lower yield. However, it is clear that the yield of Ag NCs was increased as the concentration of NaHS was 2.66×10^{-3} mM (Fig. 3*b*). The

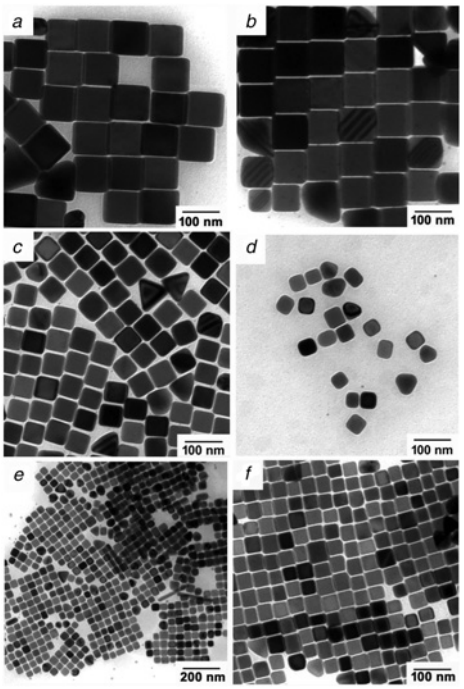

Fig. 1 *TEM images of Ag NCs prepared under different reaction temperatures*
a 60°C, the Ag NCs have an edge length of 80 nm
b 50°C, the Ag NCs have an edge length of 60 nm
c 40°C, the Ag NCs have an edge length of 45 nm
d 30°C, the Ag NCs have an edge length of 35 nm
e, f Synthesis of Ag NCs were further optimised at 30°C, at different magnifications

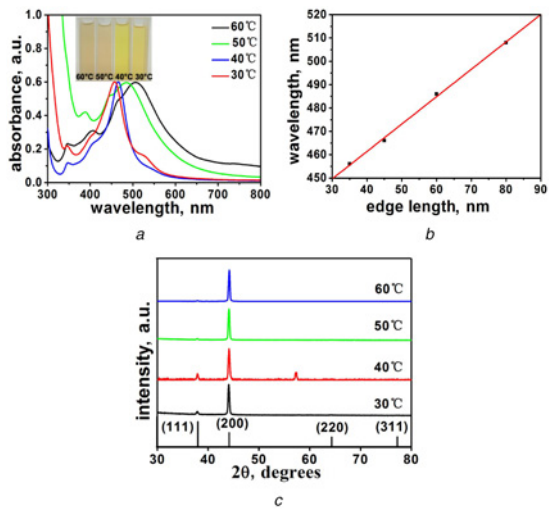

Fig. 2 *UV–Vis adsorption spectra, calibration curve and XRD patterns of Ag NCs*
a UV–Vis adsorption spectra of Ag NCs at 60, 50, 40, 30°C, respectively. The inset shows the photographs of the colloids obtained at different reaction temperatures
b Calibration curve showing the linear dependence between the major LSPR peak position and the edge length of Ag NCs
c XRD patterns of Ag NCs at 60, 50, 40, 30°C, and that of standard JCPDF 65-2871 (Ag)

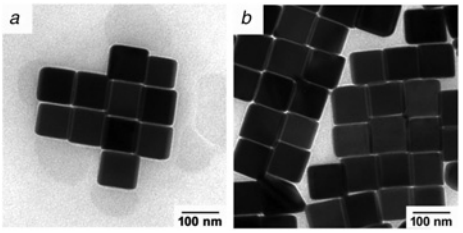

Fig. 3 *TEM images of Ag NCs as the concentration of NaHS was varied*
a 0 mM
b 2.66×10^{-3} mM
Reaction temperature was 60°C

concentration of the Ag NCs colloid was estimated according to the Beer–Lambert law to analyse the absorbance spectra [29]. Absorbance ∞ concentration (A ∞ C) under weak colloid, the red curve was higher than the black curve in Fig. 4*a*, which agreed with the TEM results in Fig. 3. Without using NaHS, AgCl of early-stage formation was dissolved and reduced to form Ag NCs [22] (Fig. 4*b* (a_1–a_3)). After using NaHS, it could help homogeneous nucleation at a suitable concentration, which might block the production of twinned seeds and polydispersed samples. As shown in Fig. 4*b* (b_1–b_3), NaHS as nucleating auxiliary agent involved in the formation of Ag NCs. As a result, Ag NCs with high yield were obtained. Effects of SH^- on Ag nucleation and the yield of Ag NCs have been systematically reported by Xia's group [14, 21].

3.3. Effects of daylight illumination: In order to investigate the roles of daylight illumination played in the preparation of Ag NCs, the experiments were conducted in the dark. As shown in Figs. 5*c* and *d*, the number of Ag NCs was relatively small, and they were mainly spherical and irregular in shape. The XRD patterns (Fig. 6) indicated the coexistence of AgCl and Ag NPs throughout the synthesis. Meanwhile, it demonstrated that AgCl

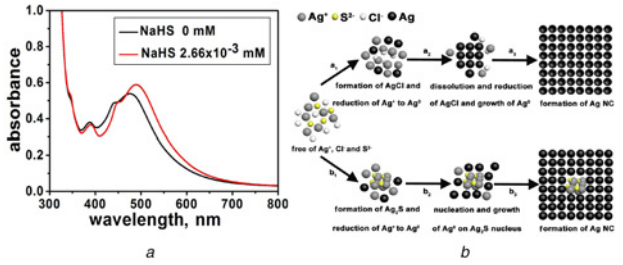

Fig. 4 *UV–Vis adsorption spectra of Ag NCs*
a UV–Vis adsorption spectra of Ag NCs under different concentration of NaHS. The red curve and black curve recorded from an aqueous suspension of the sample shown in Figs. 3*a* and *b*, respectively.
b Schematic diagram of the mechanism involved in the two kinds of formation of Ag NCs. On the one way: (a_1) formation of AgCl and reduction of Ag^+ to Ag^0; (a_2) dissolved and reduced of AgCl and growth of Ag^0; (a_3) formation of Ag NC. On the other way: (b_1) formation of Ag_2S and reduction of Ag^+ to Ag^0; (b_2) nucleation and growth of Ag^0 on Ag_2S nucleus; (b_3) formation of Ag NC

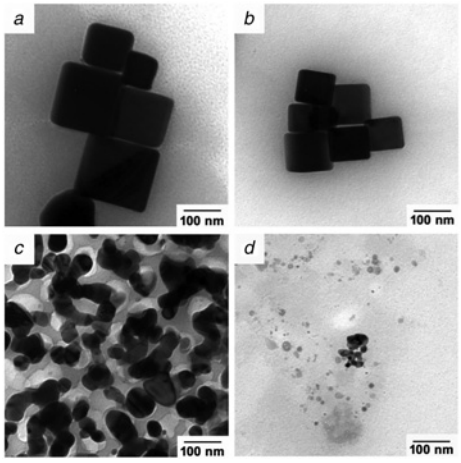

Fig. 5 *TEM images of Ag NCs prepared in the dark with different reaction temperatures*
a 60°C
b 50°C
c 40°C
d 30°C

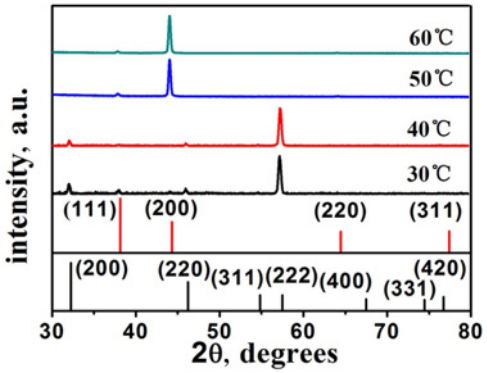

Fig. 6 *XRD patterns of Ag NCs at 60, 50, 40, 30°C in the dark (from the top to bottom), and the red curve corresponding to standard JCPDF 65-2871 (Ag), the black curve corresponding to JCPDF 31-1238 (AgCl)*

was reduced at relatively low temperature and in the dark. As the reaction temperatures were increased to 50 and 60°C, Ag NCs were prepared. These results corresponded with the XRD patterns (Fig. 6). However, their sizes were not uniform (Figs. 5*a* and *b*), compared with Figs. 1*a* and *b*. Therefore, daylight illumination is an indispensable condition for formation of Ag NCs with uniform size, especially at low reaction temperature. As a result, Ag NCs can be successfully prepared at 30°C under light irradiation owing to the coordination effects of thermal reduction and photoinduced reduction [30].

4. Conclusions: In summary, Ag NCs with uniform size and high yield were obtained under 30°C oil bath and 6 h irradiated with a daylight. It is worth emphasising that it was the coordination effects of thermal reduction and photoinduced reduction to promote the synthesis of Ag NCs at low reaction temperature. At present, the experiments of preparing Ag NCs at room temperature are undergoing in our laboratory. Further experimental study to apply these Ag NCs as outstanding substrates for SERS detection also needs to be carried out in the future.

5. Acknowledgment: This work was financially supported in part by a fund from the Scientific Research Project of Beijing Educational Committee (grant no. KM201510028008).

6 References

[1] Ahamad N., Bottomley A., Ianoul A.: 'Optimizing refractive index sensitivity of supported silver nanocube monolayers', *J. Phys. Chem. C*, 2012, **116**, (1), pp. 185–192
[2] Dubas S.T., Pimpan V.: 'Optical switch from silver nanocomposite thin films', *Mater. Lett.*, 2008, **62**, (19), pp. 3361–3363
[3] Nie S.: 'Probing single molecules and single nanoparticles by surface-enhanced Raman scattering', *Science*, 1997, **275**, (5303), pp. 1102–1106
[4] Jia H.Y., Zeng J.B., Song W., *ET AL.*: 'Preparation of silver nanoparticles by photo-reduction for surface-enhanced Raman scattering', *Thin Solid Films*, 2006, **496**, (2), pp. 281–287
[5] Lukman A.I., Gong B., Marjo C.E., *ET AL.*: 'Facile synthesis, stabilization, and anti-bacterial performance of discrete Ag nanoparticles using Medicago sativa seed exudates', *J. Colloid Interface Sci.*, 2011, **353**, (2), pp. 433–444
[6] Liang H., Wang W., Huang Y., *ET AL.*: 'Controlled synthesis of uniform silver nanospheres', *J. Phys. Chem. C*, 2010, **114**, (16), pp. 7427–7431
[7] Tang A., Qu S., Hou Y., *ET AL.*: 'One-pot synthesis, optical property and self-assembly of monodisperse silver nanospheres', *J. Solid State Chem.*, 2011, **184**, (8), pp. 1956–1962
[8] Tang A., Wang Y., Ye H., *ET AL.*: 'Controllable synthesis of silver and silver sulfide nanocrystals via selective cleavage of chemical bonds', *Nanotechnology*, 2013, **24**, (35), p. 355602
[9] Zhang Q., Li W., Moran C., *ET AL.*: 'Seed-mediated synthesis of Ag nanocubes with controllable edge lengths in the range of

doi: 10.1049/mnl.2017.0703

30–200 nm and comparison of their optical properties', *J. Am. Chem. Soc.*, 2010, **132**, (32), pp. 11372–11378
[10] Sun Y.G., Xia Y.N.: 'Shape-controlled synthesis of gold and silver nanoparticles', *Science*, 2002, **298**, (5601), pp. 2176–2179
[11] Siekkinen A.R., McLellan J.M., Chen J., *ET AL.*: 'Rapid synthesis of small silver nanocubes by mediating polyol reduction with a trace amount of sodium sulfide or sodium hydrosulfide', *Chem. Phys. Lett.*, 2006, **432**, (4–6), pp. 491–496
[12] Im S.H., Lee Y.T., Wiley B., *ET AL.*: 'Large-scale synthesis of silver nanocubes: the role of HCl in promoting cube perfection and monodispersity', *Angew. Chemie*, 2005, **44**, (14), pp. 2154–2157
[13] Wang Y., Zheng Y., Huang C.Z., *ET AL.*: 'Synthesis of Ag nanocubes 18–32 nm in edge length: the effects of polyol on reduction kinetics, size control, and reproducibility', *J. Am. Chem. Soc.*, 2013, **135**, (5), pp. 1941–1951
[14] Ruditskiy A., Xia Y.: 'Toward the synthesis of sub-15 nm Ag nanocubes with sharp corners and edges: the roles of heterogeneous nucleation and surface capping', *J. Am. Chem. Soc.*, 2016, **138**, (9), pp. 3161–3167
[15] Wiley B.J., Chen Y.C., McLellan J.M., *ET AL.*: 'Synthesis and optical properties of silver nanobars and nanorice', *Nano Lett.*, 2007, **7**, (4), pp. 1032–1036
[16] Wu Q., Liu R.Y., Shang Y.Y., *ET AL.*: 'Preparation methods of silver nanocubes', *J. Qi Lu Univ. Technol.*, 2016, **30**, (4), pp. 12–16
[17] Yu D., Yam V.W.: 'Controlled synthesis of monodisperse silver nanocubes in water', *J. Am. Chem. Soc.*, 2004, **126**, (41), pp. 13200–13201
[18] Chen H., Wang Y., Dong S.: 'An effective hydrothermal route for the synthesis of multiple PDDA-protected noble-metal nanostructures', *Inorg. Chem.*, 2007, **46**, (25), pp. 10587–10593
[19] Fan F.R., Liu D.Y., Wu Y.F., *ET AL.*: 'Epitaxial growth of heterogeneous metal nanocrystals: from gold nano-octahedra to palladium and silver nanocubes', *J. Am. Chem. Soc.*, 2008, **130**, (22), pp. 6949–6951
[20] Zhang Q., Huang C.Z., Ling J., *ET AL.*: 'Silver nanocubes formed on ATP-mediated nafion film and a visual method for formaldehyde', *J. Phys. Chem. B*, 2008, **112**, (51), pp. 16990–16994
[21] Zhang Q., Li W., Wen L.P., *ET AL.*: 'Facile synthesis of Ag nanocubes of 30 to 70 nm in edge length with CF(3)COOAg as a precursor', *Chemistry*, 2010, **16**, (33), pp. 10234–10239
[22] Zhou S., Li J., Gilroy K.D., *ET AL.*: 'Facile synthesis of silver nanocubes with sharp corners and edges in an aqueous solution', *ACS Nano*, 2016, **10**, (11), pp. 9861–9870
[23] Zhou H., Zhang Z., Jiang C., *ET AL.*: 'Trinitrotoluene explosive lights up ultrahigh Raman scattering of nonresonant molecule on a top-closed silver nanotube array', *Anal. Chem.*, 2011, **83**, (18), pp. 6913–6917
[24] Wilson R., Bowden S.A., Parnell J., *ET AL.*: 'Signal enhancement of surface enhanced Raman scattering and surface enhanced resonance Raman scattering using in situ colloidal synthesis in microfluidics', *Anal. Chem.*, 2010, **82**, (5), pp. 2119–2123
[25] Schlucker S.: 'SERS microscopy: nanoparticle probes and biomedical applications', *ChemPhysChem*, 2009, **10**, (9–10), pp. 1344–1354
[26] Preciado-Flores S., Wheeler D.A., Tran T.M., *ET AL.*: 'SERS spectroscopy and SERS imaging of shewanella oneidensis using silver nanoparticles and nanowires', *Chem. Commun.*, 2011, **47**, (14), pp. 4129–4131
[27] Willets K.A.: 'Surface-enhanced Raman scattering (SERS) for probing internal cellular structure and dynamics', *Anal. Bioanal. Chem.*, 2009, **394**, (1), pp. 85–94
[28] Chang Y.M., Lu I.T., Chen C.Y., *ET AL.*: 'High-yield water-based synthesis of truncated silver nanocubes', *J. Alloys Compd.*, 2014, **586**, pp. 507–511
[29] Jin R., Wu G., Li Z., *ET AL.*: 'What controls the melting properties of DNA-linked gold nanoparticle assemblies', *J. Am. Chem. Soc.*, 2003, **125**, (6), pp. 1643–1654
[30] Yu H., Zhang Q., Liu H., *ET AL.*: 'Thermal synthesis of silver nanoplates revisited: a modified photochemical process', *ACS Nano*, 2014, **8**, (10), pp. 10252–10261